

Refereed Proceedings

The 13th International Conference on

Fluidization - New Paradigm in Fluidization

Engineering

Engineering Conferences International

Year 2010

HYDRODYNAMICS OF
UNCONVENTIONAL FLUIDIZED
BEDS: SOLIDS FLOW PATTERNS
AND THEIR INFLUENCE ON
MIXING/SEGREGATION OF A
LARGE FLOTSAM PARTICLE IN A
BED OF FINER SOLIDS

Roberto Solimene*

Paola Ammendola, Giovanna Ruoppolo[†]

Riccardo Chirone[‡]

*Istituto di Ricerche sulla Combustione – CNR, solimene@irc.cnr.it

[†]Istituto di Ricerche sulla Combustione – CNR

[‡]Istituto di Ricerche sulla Combustione – CNR

This paper is posted at ECI Digital Archives.

http://dc.engconfintl.org/fluidization_xiii/114

HYDRODYNAMICS OF UNCONVENTIONAL FLUIDIZED BEDS: SOLIDS FLOW PATTERNS AND THEIR INFLUENCE ON MIXING/SEGREGATION OF A LARGE FLOTSAM PARTICLE IN A BED OF FINER SOLIDS

Roberto Solimene, Paola Ammendola, Giovanna Ruoppolo, Riccardo Chirone
Istituto di Ricerche sulla Combustione – CNR
Piazzale Tecchio, 80
80125 Napoli Italy
T: +390817682237; F: +390815936936; E: solimene@irc.cnr.it

ABSTRACT

Gross solids circulation of solid phase and its influence on mixing/segregation of a large flotsam particle in beds of finer solids in unconventional fluidized beds has been investigated. A tapered two-dimensional fluidization column and a fluidization column equipped with a diverging cone as gas distributor have been adopted. The hydrodynamics of the gas-solid suspension in the two apparatus has been qualitatively assessed by visual observation and the trajectories of the centre-of-gravity of large flotsam particles have been evaluated to assess the extent of mixing/segregation.

INTRODUCTION

Gross solids circulation (i.e. reactor scale vortices) and intimate gas-solids contacting typical of conventional fluidization can be required in many industrial applications. For instance, during combustion and gasification of high-volatile matter fuels (1-4), gross solids circulation can significantly limit the self-segregation of fuel particles during devolatilization without reducing the intimate gas-solid contact necessary to char burn-out. During drying of wet granules of pharmaceutical substances (5), gross solids circulation is also required to reduce agglomeration phenomena and channelling.

Gross solids circulation can be substantially generated by an uneven distribution of bubbles inside the bed. Merry and Davidson (6) suggested to induce bed-height scale vortices by means of an uneven distribution of fluidizing gas flow through the distributor plate. These authors individuated bed solids circulation evocating the “Gulf Stream” circulation. The gas-solid hydrodynamic pattern of the “Gulf Stream” circulation” can be also achieved with unconventional fluidized bed configurations: i) tapered fluidized beds (7-9); ii) conventional fluidized beds with an unconventional distributor. Though a relative extensive literature on solids flow patterns present in these configurations is available, a comprehensive understanding of the influence of gross solids circulation on mixing/segregation of large flotsam particles is still lacking.

The aim of this work is the study of hydrodynamics of two lab-scale cold unconventional fluidized beds: a fluidized bed with a diverging cone as gas distributor and a 2-D tapered fluidized bed. The hydrodynamics of the gas-solid suspension in the two

apparatus was investigated by visual observation. The hydrodynamic characterization was mainly carried out by tracking the trajectory, on one hand, of dye-coloured particles to study the solids flow patterns and, on the other, of a large flotsam particle to study the mixing/segregation phenomena varying: i) fluidization velocity; ii) type, size and amount of bed material; iii) type and size of large flotsam particle.

EXPERIMENTAL

Apparatus and experimental procedures

Fluidized bed with a diverging cone as gas distributor: The 3-D experimental apparatus shown in Fig. 2, basically consists of a fluidization column equipped with a diverging cone as gas distributor and it represents a cold model of a pilot-scale hot gasifier (10). The fluidized bed column (I.D. 120 mm) is made of Plexiglas and is 1 m high. The conical distributor is 0.1 m high with an apex angle of 41°. The lateral surface of the cone is equipped with 32 evenly-distributed nozzles of 6 mm diameter. The fluidizing gas is fed to the column through the nozzles of the distributor. The gas flow is controlled using a set of high-precision rotameters. The visual observation of the bed during the experiments was also recorded by a high-resolution video-camera.

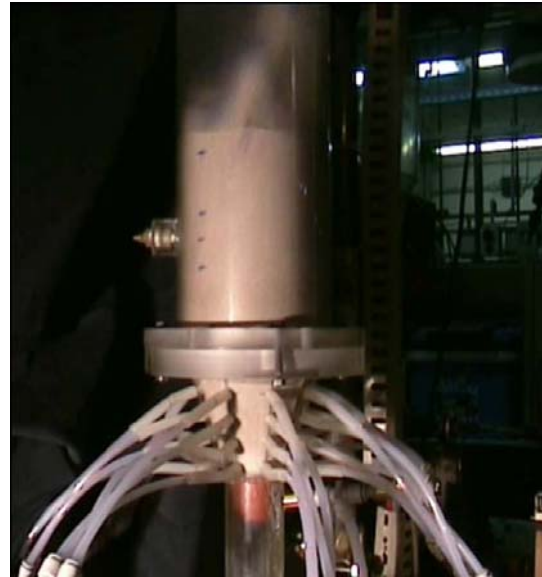


Figure 1 – Image of the fluidization column equipped with a diverging cone as gas distributor.

The experiments have been characterized in terms of superficial gas velocity, bed material and bed inventory. Three different bed inventories are adopted: 1.35, 1.95 and 2.75 kg. The superficial gas velocity has been varied between 0.17 and 0.29 m/s. The images recorded during the tests have been then processed in order to analyze the motion of solid and diluted phases and to estimate the wall downward flotsam velocity.

Tapered 2-D fluidized bed:

The experimental apparatus, sketched in Fig. 2, consists of a two-dimensional tapered fluidization column, a gas flow controller system, a

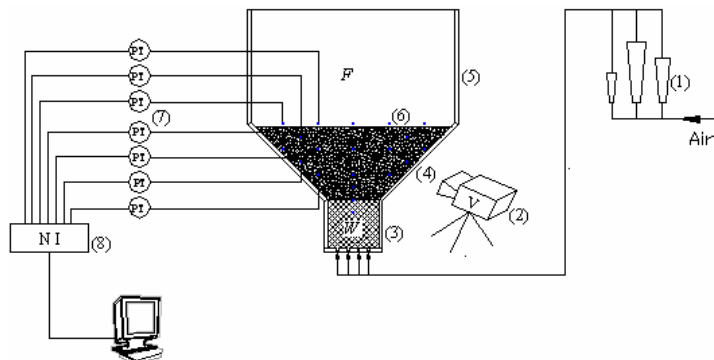


Figure 2 – Two-dimensional tapered fluidization column: (1) rotameters; (2) video camera; (3) wind-box; (4) bed; (5) freeboard; (6) pressure taps, (7) pressure transducers; (8) A/D conversion board (National Instruments).

video camera, a set of pressure transmitters, and a data acquisition unit. The two-dimensional fluidization column is 0.950 m high, 0.018 m thick with width variable axially from 0.2 to 0.48 m. The fluidization column is totally made of Plexiglas including front and rear walls to visualize the gas-solid suspension. The fluidizing gas is fed to the bottom of the column, flowing into the wind-box, 0.2 m high and 0.2 m wide, filled by hollow cylinders to even the flow. The gas, then, percolates through a low-pressure drop distributor plate basically made of a stain-steel mesh. The inclination of the lateral walls of the fluidized bed with respect to the vertical axis is 26° (apex angle 52°). The freeboard is wide 0.48 m and high 1 m. The gas flow controller system is based on the use of a set of high-precision rotameters. A high-rate video camera was used to record the fluidized bed during the experiments. The experiments have been characterized in terms of U_{bottom} and of bed inventory. Different bed inventories are adopted 0.5, 1 and 1.5 kg. The superficial gas velocity at the bottom of the bed, U_{bottom} , has been varied between 0.1 and 3 m/s. The study has been focused on the visual observation of the motion of solid and diluted phases as well as of a large flotsam particle. The acquired images have been analyzed by means of an "ad hoc" procedure to determine the coordinates of the centre-of-gravity of large flotsam particles in order to follow the trajectories of the particle along the column.

Materials and diagnostic techniques

Silica sand sieved in size range 300-400 μm ($U_{\text{mf}}=0.1$ m/s at 25°C , $\rho_{\text{particle}}=2600$ kg/m^3) has been used in tests with the tapered two-dimensional fluidized bed. Silica sand sieved in size range 100-400 μm ($U_{\text{mf}}=0.05$ m/s at 25°C , $\rho_{\text{particle}}=2600$ kg/m^3) and commercial γ -alumina (PURALOX SCCA-150/200, SASOL) in size range 150-200 μm ($U_{\text{mf}}=0.02$ m/s at 25°C , $\rho_{\text{particle}}=1800$ kg/m^3) have been used in the fluidization column equipped with the diverging cone as gas distributor. The flotsam particle adopted in the tapered fluidization column consists of cork particle (cylindrical shape, 24 mm OD and 16 mm thick, $\rho_{\text{particle}}=290$ kg/m^3), whereas of wood pellet char (cylindrical shape, 5.5 mm OD and 6 mm thick, $\rho_{\text{particle}}=250$ kg/m^3) charged with a char/bed ratio of 3%wt in the fluidization column equipped with the diverging cone as gas distributor. A sample of bed material black-coloured has been adopted as solids tracer. The experiments have been carried out at ambient conditions using technical air as fluidizing gas in both apparatus. The visual observation in the two apparatus is accomplished by means of a high-speed, highly light-sensitive mega-pixel CMOS camera interfaced to a computer and controlled with an image processing software.

RESULTS AND DISCUSSION

Fluidized bed with a diverging cone as gas distributor: A qualitative assessment of the hydrodynamics of gas-solid suspension in the fluidization column equipped with a diverging cone as gas distributor, obtained by a visual observation of solids tracer, highlighted the presence of two regions for all the investigated experimental conditions: i) the first one corresponds to the central region of the bed mainly characterized by the presence of bubbles, which induce the upward solids motion; ii) the second one is the region surrounding the central one and it is characterized by the absence of bubbles and downward motion of bed particles. The particles ejected on the bed surface are transferred from the first to the second region, where they descend along the lateral

walls toward the conical distributor, inducing a gross circulation in the solid phase. The influence of the hydrodynamic pattern of bed solids on the mixing/segregation of wood char particles has been investigated following their trajectory nearby the column wall, for different operating conditions. Figure 3 reports the trajectory nearby the column wall of some char particles obtained at different times using alumina as bed material (bed inventory=1.95 kg) at lowest gas velocity (0.17 m/s, $U-U_{mf}=0.16$ m/s). The visual observation of the bed highlights the general occurrence of solid mixing in the bed without segregation of char particles on the bed surface for the highest bed inventory (2.75 kg), whatever the gas velocity excess. On the contrary, a rather limited segregation of char on the bed surface has been observed for the other two bed inventories (1.35 and 1.95 kg) only for the lowest gas velocity excess (0.12 m/s). The image processing makes possible the estimation of the wall downward flotsam velocity corresponding to the different operating conditions. In Fig. 4 the wall downward flotsam velocities obtained using the two bed materials as function of $U-U_{mf}$ for different bed inventories are reported. As expected, the downward velocity for both materials increases with the increase of $U-U_{mf}$ whatever the bed inventory, even if the effect is more evident for the lowest bed inventory. At a pre-set $U-U_{mf}$ the downward velocity increases as bed inventory increases, the effect being higher for the lowest gas velocity excess. These evidences could be related to the beneficial effect of the bubble coalescence promoted by high bed inventories and high $U-U_{mf}$. The comparison between the two bed materials shows that, at pre-set bed inventory and $U-U_{mf}$, higher downward velocities have been measured for the γ -alumina characterized by a lower particle densities than the silica sand. This result could be explained on the basis of the reduced difference of density between the bed and the flotsam material for the γ -alumina with respect to the silica sand. The correlation between the visual observation of char mixing/segregation and the estimated values of downward velocity shows that the occurrence of char segregation, observed for two lowest bed inventories (1.35 and 1.95 kg) and the lowest $U-U_{mf}$ (0.12 m/s), is probably related to a limited action of bubbles, which, in turn, determines in a downward velocity lower than 0.02 m/s.

Tapered 2-D fluidized bed: A qualitative assessment of the hydrodynamics of gas-solid

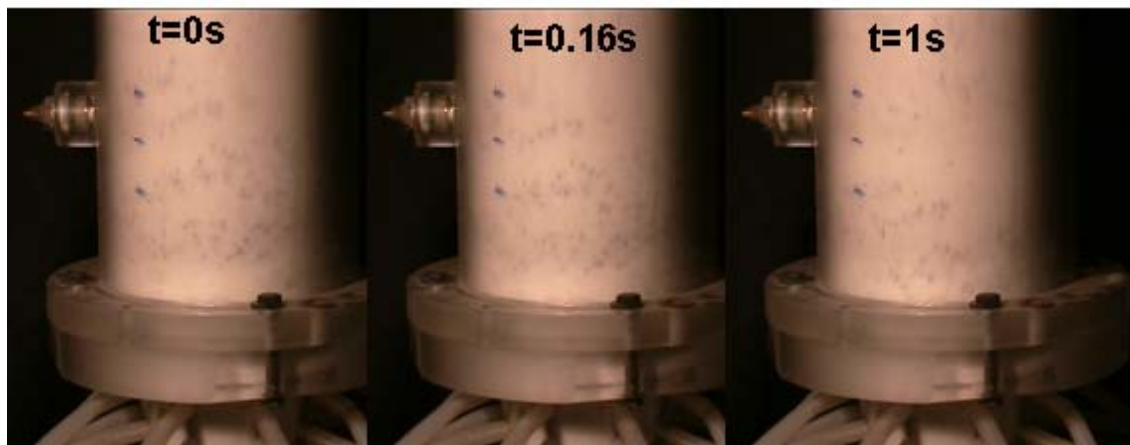


Figure 3 – Wall trajectory of some char particles obtained at different times. Bed material: alumina (150-200 μm); fluidization velocity: 0.17 m/s ($U-U_{mf}=0.16$ m/s, bed inventory=1.95 kg).

suspension in the tapered two-dimensional fluidized bed pointed out a hydrodynamic behaviour similar to that observed in the previous described 3-D experimental apparatus. As matter of fact, the visualization of the gas-solid suspension in the 2-D fluidization column allowed to evaluate the spatial extension of the regions characterized by different hydrodynamic behaviours. In particular, it was possible to individuate: i) an A-Domain localized in the central region of the bed and characterized by the presence of rising gas pockets and, in turn, by a net upward mass flow rate of solids; ii) a B-Domain surrounding the central one and characterized by the absence of bubbles and by a constant downward flux of particles. Along the boundary between A-Domain and B-Domain the descending particles in the B-Domain are entrained into the solid flux of the A-Domain establishing gross circulation in the solid phase. Differently from the observation in the 3-D fluidization column equipped with a diverging cone as distributor, for low values of U_{bottom} it can be also recognized a S-Domain region surrounding the B-Domain and extended until to the walls of the column. The S-Domain remains mainly defluidized and the solid phase appears stagnant. The extension of this region progressively decreases until to vanish at large values of U_{bottom} and for low values of bed inventory.

The influence of the observed hydrodynamic patterns on the mixing/segregation of a large flotsam particle has been investigated following the trajectory of the centre-of-gravity of a cork particle inside the bed varying U_{bottom} and the bed inventory. Figure 5 reports the co-ordinates (y,x) of the centre-of-gravity of a cork particle measured in typical sequences of images acquired at 50 fps for 60 s, together with a snapshot acquired during the video recordings for three different values of U_{bottom} . The bed material and inventory were silica sand (300-400 μm) and 1 kg, respectively. It is worth to note that: i) it is assumed as centre of y and x axis the midpoint of the plate distributor; ii) the solid line, present in Fig. 5, represents the lateral walls and the distributor plate of the fluidization column. The trajectories show that the flotsam particle move along the column describing vortices of different scales approximately symmetric with y axis. According to the bed solids motion, the particle rises in the A-Domain and descends in the B-Domain. Once it is ejected above the bed it falls down at right or left with respect to the y axis. Increasing U_{bottom} it can be observed that the dimension of vortices increases as well as the depth penetration of the flotsam particle inside the bed. The image analysis has been further carried out to evaluate main hydrodynamics features of the motion of flotsam particles as a function of U_{bottom} and of bed inventory

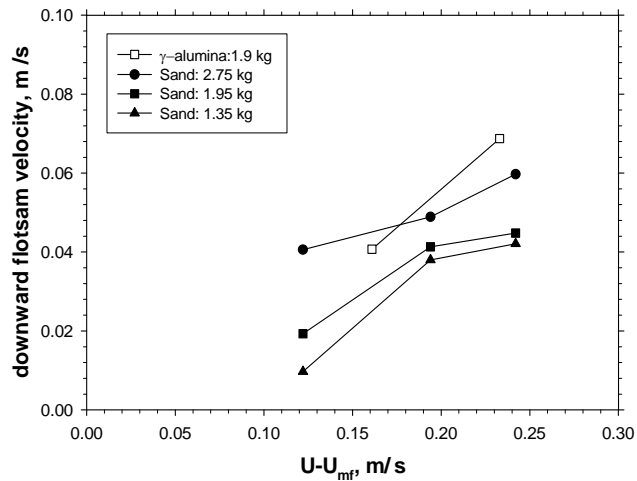


Figure 4 – Wall downward flotsam velocity as a function of $U - U_{mf}$ for different bed inventories.

(m_{bed}): i) the time-averaged upward velocity (v_yA) in the A-domain; ii) the time-averaged downward velocity (v_yB) in B-Domain; iii) the fractional time intervals (x_tA , x_tB , x_tC) during which the flotsam particle is present in the A-Domain, in the B-Domain and in the splash zone, respectively.

Figure 6 reports data obtained during tests with cork flotsam particle: i) v_yA , v_yB , x_tA , x_tB , x_tC as a function of U_{bottom} keeping constant the bed inventory (1 kg); ii) v_yA , v_yB , x_tA , x_tB , x_tC as a function of m_{bed} keeping constant U_{bottom} (1.9 m/s). It can be observed

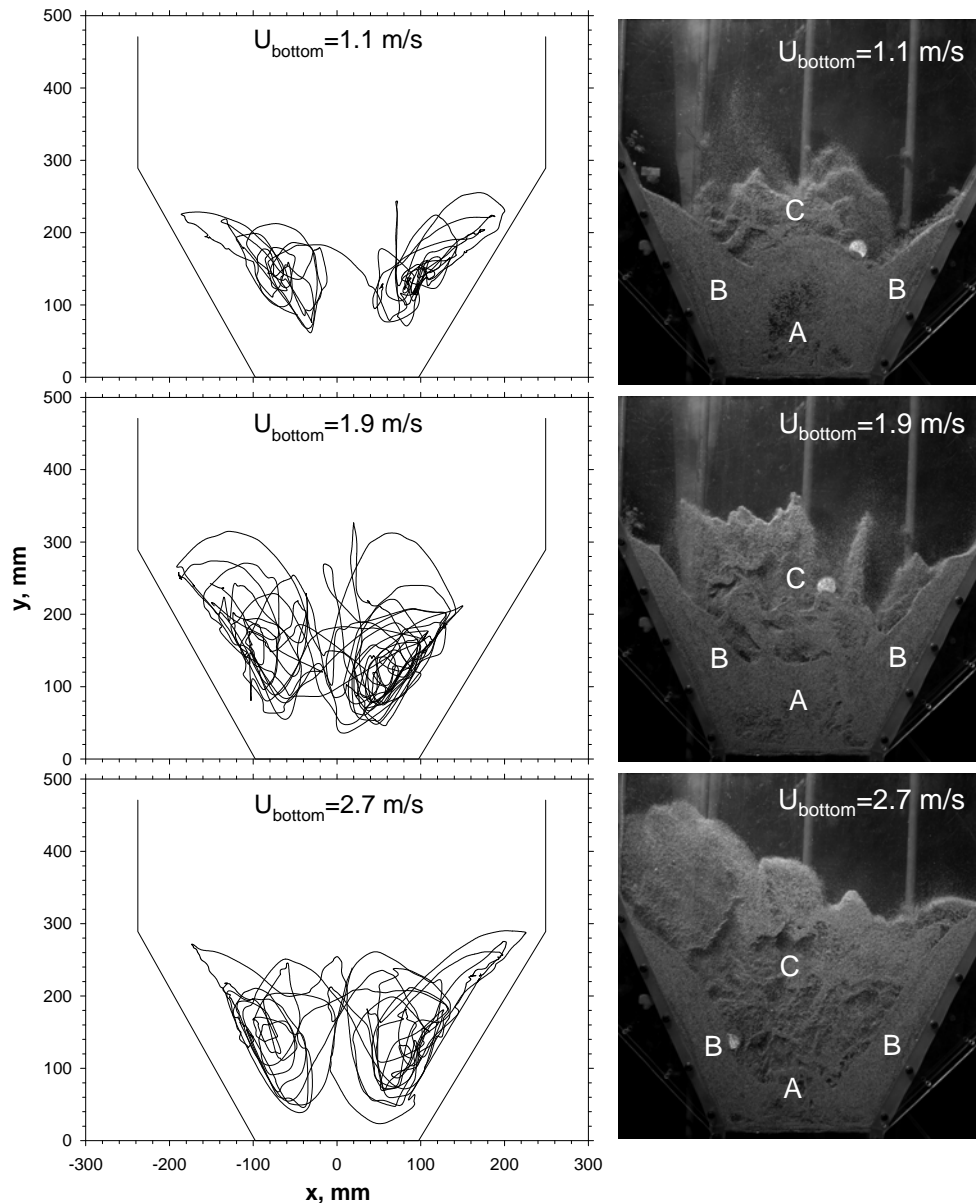


Figure 5 – Trajectories of centre-of-gravity of cork particle measured in typical sequences of images acquired at 50 fps for 60 s, together with snapshots of 2-D tapered fluidized bed for different values of U_{bottom} . A: A-Domain; B: B-Domain; C: splash zone. Bed material: silica sand (300-400 μm); bed inventory=1 kg.

that increasing U_{bottom} : i) x_{tA} remains substantially constant (about 21%); ii) x_{tB} and x_{tC} decreases and increases, respectively, to level off for values larger than 1.9 m/s; iii) v_{yA} , v_{yB} increases and decreases, respectively. Increasing m_{bed} it is worth note that: i) x_{tA} and x_{tC} data points highlight a non monotonic trend with the presence of a minimum and a maximum value, respectively, at m_{bed} equal to 1 kg, ii) x_{tB} remains substantially constant (about 56%); iii) v_{yA} presents a non monotonic behaviour with a maximum at m_{bed} equal to 1 kg; iv) v_{yB} monotonically decreases. The influence of the U_{bottom} on the time-averaged velocities v_{yA} and v_{yB} is rather trivial: larger the fluidization velocity larger is the gross solids circulation in the bed. On the other hand, increasing U_{bottom} x_{tA} does not change probably because the increase of the upward velocity is compensated by an increase of the height of A-Domain, whereas x_{tC} increases because of larger height reached by the flotsam particle in the splash zone, but this effect is, however, limited by the decrease of the fluidization velocity along the tapered column. The initial decrease of x_{tB} with U_{bottom} is probably due to the increase of the absolute value of downward velocity in the B-Domain, but this effect is partially reduced by an increase of the depth penetration of the flotsam particle inside the bed.

As regards the influence of the bed inventory on hydrodynamics features of the motion of flotsam particles, it can be speculated that increasing m_{bed} : i) the part of fluidizing gas flow rate, that percolates in the B-Domain, increases improving the flow ability of solids particles in this region and, as consequence, causing a monotonic decrease of v_{yB} ; ii) on one hand, gas-solid suspension present in A-Domain becomes denser and denser and, in turn, the momentum transferred from the gas-solid suspension to the flotsam particle raises, on the other less and less gas fluidizing flow rate percolates in A-

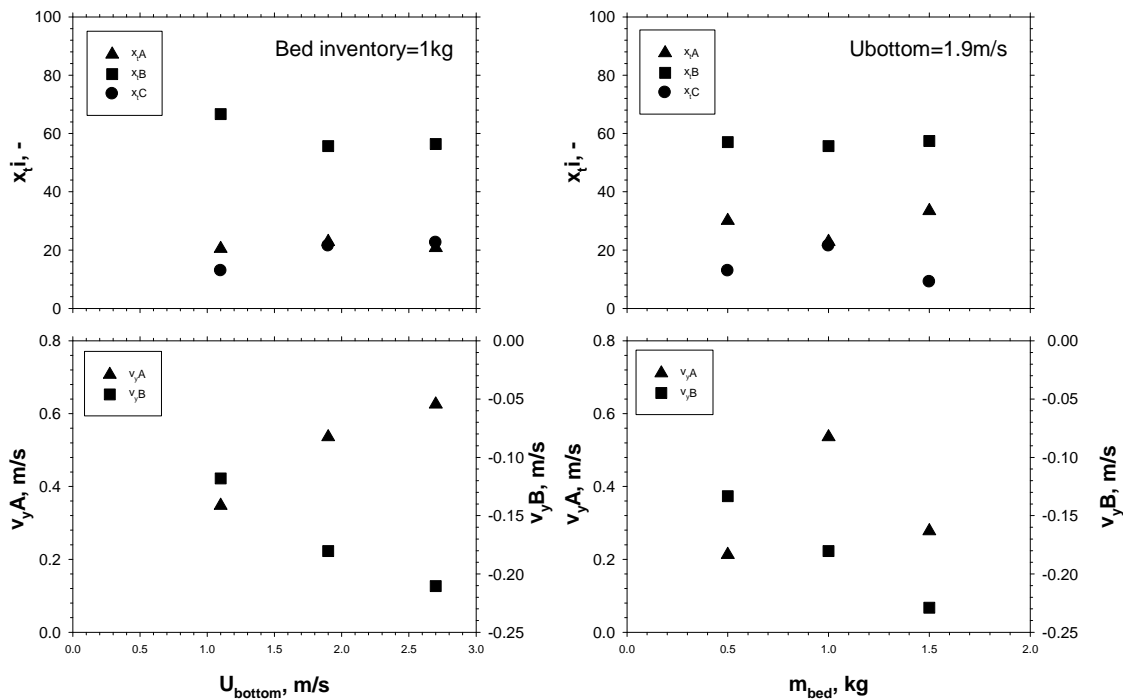


Figure 6 – Main hydrodynamics features of the motion of flotsam particles as a function of U_{bottom} and of bed inventory.

Domain reducing the energy input to this region, these opposite effects could explain the non monotonic trend of v_yA , x_tA and x_tC ; iii) x_tB remains substantially constant as the increase of the absolute value of downward velocity is balanced by the increase of depth penetration of the flotsam particle inside the bed.

CONCLUSIONS

A preliminary hydrodynamic characterization of solids motion in a tapered two-dimensional fluidization bed and in a fluidized bed equipped with a diverging cone as gas distributor has been successfully achieved by visual observation. Both fluidized beds are characterized by upward and downward solids motion in the central and in the lateral part of bed, respectively. The trajectories of large flotsam particles have been analyzed to study the mixing/segregation phenomena inside the two tested apparatus for different operating conditions. Tests carried out in the fluidized bed equipped with a diverging cone as gas distributor highlight the absence of segregation of flotsam particles for most of the operating conditions investigated and, in particular, once the wall downward velocity of flotsam particles exceeds 0.02 m/s. Tests carried out in the tapered two-dimensional fluidized bed underline that the flotsam particle spends about 50-60% of time moving downwards at a relatively large absolute value of downward velocity (about 0.1-0.25 m/s) and only about 20% above the bed. The results obtained in both apparatus are encouraging for successful applications of these kind of unconventional fluidized beds in processes where large flotsam particles have to be in touch with a bed of finer solids.

REFERENCES

- 1) Steiner C. Selinger A., in Proceedings of the 9th International Conference on Circulating Fluidized Beds, Werther, J., Nowak, W., Wirth, K.-E., Hartge, E.-U., Eds., TuTech Innovation: Hamburg, 621, 2008.
- 2) Nienow A. W., Rowe P. N., in Proceeding of the 1st International Symposium on Materials and Energy from Refuse, 131, 1976.
- 3) Bruni G., Solimene R., Marzocchella A., Salatino P., Yates J. G., Lettieri P., Fiorentino M., Powder Technology, 128, 11, 2002.
- 4) Solimene, R., Marzocchella A., Salatino P., Powder Technology, 173, 79, 2003.
- 5) Wormsbecker M., van Ommen R., Nijenhuis J., Tanfara H., Pugsley T., Powder Technology, 194, 115, 2009.
- 6) Merry J. M. D., Davidson J. F., Transactions of Institution of Chemical Engineers, 51, 361, 1973.
- 7) Schaafsma S. H., Marx T., Hoffmann A. C., Chemical Engineering Science, 61, 4467, 2006.
- 8) Bahramian A., Kalbasi M., Olazar M., International Journal of Chemical Reactor Engineering, 7, A60, 2009.
- 9) Gernon T. M., Gilbertson M. A., Sparks R. S. J., Field M., Journal of Volcanology and Geothermal Research, 174, 49, 2008.
- 10) Miccio F., Piriou B., Ruoppolo G., Chirone R., Chemical Engineering Journal, 154, 369, 2009.